Selective Production of Light Oil by Biomass Pyrolysis with Feedstock-Mediated Recycling of Heavy Oil

ARTICLE *in* ENERGY & FUELS · SEPTEMBER 2011

Impact Factor: 2.79 · DOI: 10.1021/ef2011673

5 AUTHORS, INCLUDING:

Shinji Kudo
Kyushu University
44 PUBLICATIONS **259** CITATIONS
SEE PROFILE

Koyo Norinaga
Kyushu University
96 PUBLICATIONS **1,222** CITATIONS
SEE PROFILE

Jun-ichiro Hayashi
Kyushu University
201 PUBLICATIONS **3,652** CITATIONS
SEE PROFILE

energy&fuels

ARTICLE

pubs.acs.org/EF

Selective Production of Light Oil by Biomass Pyrolysis with Feedstock-Mediated Recycling of Heavy Oil

Yong Huang, Shinji Kudo, Koyo Norinaga, Masaki Amaike, and Jun-ichiro Hayashi*

Institute for Materials Chemistry and Engineering, Kyushu University, 6-1, Kasuga Koen, Kasuga 816-8580, Japan

ABSTRACT: This paper proposes pyrolysis of biomass with recycling of a heavier portion of bio-oil [heavy oil (HO)] and reports results of the experimental simulation of this process, employing chipped cedar as not only the feedstock but also the sorbent/carrier of HO. Repetition of 10 pyrolysis runs in sequence simulated recycling of HO. In the *n*th run, HO-loaded cedar that had been prepared in the $(n-1)$th run was pyrolyzed at 500 °C. The volatiles, i.e., gas, steam, light oil (LO), and HO, were formed and sent to the HO sorber, in which fresh cedar sorbed HO selectively. The resultant HO-loaded cedar was subjected to the pyrolysis in the $(n+1)$th run. HO loading on the cedar became steady around 0.4 kg of HO/kg of dry cedar. Recycled HO was converted mainly by self-pyrolysis with once-through conversion of about 40%. Conversion of the recycled HO resulted in increases in char and LO yields without significant increases in the gas and water yields. The HO recycling increased the LO yield from 0.16 to 0.26 kg/kg of dry cedar (excluding water). LO from the last run was highly volatile that 99.8 wt % of its portion was evaporated in heating to 250 °C. The LO consisted mainly of compounds with a carbon number (number of carbon atoms per molecule) of 1−12. The proposed pyrolysis thus enabled selective production of LO with full recycling of HO.

1. INTRODUCTION

1.1. Problems in Thermal and Catalytic Conversion of Bio-oil Arising from Its Nature. Pyrolysis is the most popular way to convert biomass to crude liquid, which is termed bio-oil. Fast pyrolysis with a heating rate over 10^2 °C s^{-1} is effective for increasing and maximizing the bio-oil yield even to 70 wt % feedstock, including water.[1] Comprehensive reviews are available on the fast pyrolysis of biomass and properties/applications of bio-oil.[2−7] The most popular application of bio-oil is use as a boiler fuel alternative to petroleum-derived heavy fuel oil,[4] while technologies have been developed toward use of bio-oil as fuels applicable to diesel engines and turbines.[4] In such applications, a particular nature of general bio-oil, that is, the presence of heavy oil (HO) with a substantially high content, causes difficulties.

Simple heating or distillation under normal pressure of bio-oil generally leaves 20−50 wt % nonvolatile solid residue, termed coke or char.[2,5,8] Analyses, such as size-exclusion chromatography (SEC) and matrix-assisted laser desorption ionization mass spectrometry (MALDI−MS), reveal the presence of components having a molecular mass over 1000 with an appreciable content in bio-oil.[8,9] Such heavy components contribute to relatively high viscosity of bio-oil,[10,11] which is not preferred in its feeding to the combustor or other types of reactors.

Steam reforming is a potential application of bio-oil, because using it instead of solid parent biomass has some advantages.[12] A number of studies on catalytic steam reforming[12−18] have been reported. The most difficult technical problem seems to be coke formation that induces catalyst deactivation. High-molecular-mass components of bio-oil are responsible for coke formation as well as that of soot in reforming,[19] while others, such as phenol derivatives, furans, and ketones, may also be involved in the coke formation.[20] Attempts have been made for suppressing coking and catalyst deactivation by dilution of bio-oil with methanol,[14] selective use of the water phase of bio-oil,[15,18] application of a fluidized-bed reformer or two-staged reformer,[13,15] and application of a steam/carbon molar ratio of 5 or even higher.[12−18] However, it seems to be difficult to solve the coking and related problems only by improvements of the catalyst and reactor configuration, unless coke precursors are removed effectively prior to the steam reforming. Cracking-based upgrading of crude bio-oil has been studied under catalytic and noncatalytic conditions,[21−24] but the coking of bio-oil is significant, in particular, with use of acidic catalysts, such as zeolites and fluid catalytic cracking (FCC) catalysts.

Thermal conditioning[25] is a simple but effective way to reduce the content of coke precursors including a heavy portion of bio-oil by converting it into lighter oil, although coke formation will be inevitable if the thermal condition is severe enough to produce the lighter oil. Bertero and co-workers[25] prepared a bio-oil by pyrolyzing pine sawdust and heated the produced oil to 350−550 °C, while vapor formed from the oil was *in situ* carried away by the thermal conditioner. This thermal conditioning successfully reduced the content of coke precursors, such as phenolic compounds and high-molecular-mass compounds, decreasing the Conradson carbon residue (CCR) content of the oil, which is a measure for the coke-forming potential, by more than $^2/_3$. The results reported by Bertero and co-workers[25] suggest the possibility of great improvement of the quality of bio-oil in terms of coke-forming potential (in other words, volatility), if a heavier portion of bio-oil is heat-treated repeatedly until being converted into a lighter portion in a reasonable way.

Special Issue: 2011 Sino-Australian Symposium on Advanced Coal and Biomass Utilisation Technologies

Received: August 2, 2011
Revised: September 12, 2011
Published: September 12, 2011

dx.doi.org/10.1021/ef2011673 | *Energy Fuels* 2012, 26, 256–264

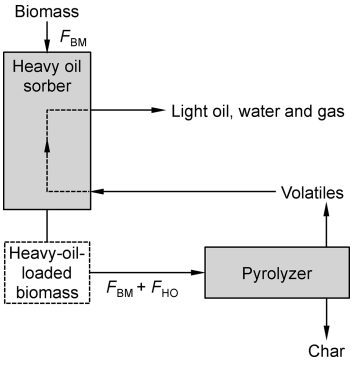

Figure 1. Conceptual diagram of biomass pyrolysis with HO recycling.

1.2. Proposal of Pyrolysis with HO Recycling. This paper proposes the pyrolysis of biomass with recycling of a heavier portion of bio-oil, hereafter termed HO, using the biomass feedstock as the recycling medium, in other words, the carrier of the HO. The primary purpose of the HO recycling is selective production of light oil (LO) without separated upgrading processes. Figure 1 shows a conceptual diagram of the process that was experimentally simulated in this study. In the proposed process, the HO, together with the LO, steam, and noncondensable gas, is sent from the pyrolyzer to the HO sorber. In the sorber, feedstock biomass captures the HO by condensation, adsorption, and/or absorption (i.e., sorption), while the LO is allowed to escape from the sorber and then sent to condensers. The feedstock biomass loaded with the HO is fed to the pyrolyzer. The HO is thus recycled, being retained and carried by the feedstock.

The HO, once condensed to liquid or solid, will be converted into char to amore or less extent during reheating to 400 °C or higher temperature, even if it is heated alone.[2,5,8] In addition to this, contact between the macromolecular matrix of the feedstock and HO can potentially enhance the pyrolysis of either of these two or both. Bio-oil is generally rich in hydroxylic functionalities, which interact with those of macromolecules, forming hydrogen bonds. Such hydrogen bonds can induce dehydration condensation between the hydroxyls enhancing char formation, i.e., co-carbonization. On the other hands, the HO with polar functionalities, such as carbonyls and ethers, as well as hydroxyls, can plasticize the macromolecular network and promote its degradation, forming more bio-oil. Although little is known about characteristics and the mechanism of the co-pyrolysis of the HO and parent biomass, it is expected that the proposed HO recycling realizes the production of LO, char, and gas without discharging the HO.

If the HO is converted into char, LO, and/or noncondensable gas at an overall conversion, X_{HO}, the feeding rate of the recycled HO at steady state, F_{HO}, is given by

$$F_{HO} = \frac{Y_{HO,0}}{X_{HO}} F_{BM} \quad (1)$$

where F_{BM} and $Y_{HO,0}$ are the feeding rate of the feedstock biomass and the HO yield from the pyrolysis of the feedstock alone, respectively. This equation is derived directly from the following material balance equation with respect to the HO, assuming that X_{HO} is steady and that the formation of the HO from the feedstock biomass and the conversion of the recycled HO are independent of each other:

$$F_{HO} = F_{BM} Y_{HO,0} + (1 - X_{HO}) F_{HO} \quad (2)$$

Continuous operation of this process requires that F_{HO}/F_{BM} be below the maximum capacity of the biomass for holding the HO. Otherwise, particles or chips of the feedstock form agglomerates in the sorber and also allow for a more or less portion of the HO to escape from the sorber. It is impossible to predict the HO holding capacity of a given biomass feedstock from its physical/chemical properties, and therefore, it is necessary to know the experimental capacity under a condition simulating the process, as illustrated in Figure 1. The composition and yield of the LO depend upon this ability, as well as the pyrolysis conditions. Equation 2 also means that X_{HO} must be higher than a certain degree. Too small of X_{HO} may break down the concept of HO recycling.

In this study, the proposed pyrolysis process was simulated experimentally by repeating cycles of pyrolysis of HO-loaded biomass and sorption of the HO, the details of which will be reported later. The primary purpose of this study was to examine the possibility of continuous operation of the pyrolysis based on $Y_{HO,0}/X_{HO}$. The secondary purpose was to investigate the effectiveness of the proposed process on the yield of the light bio-oil and its quality in terms of volatility and molecular composition.

2. EXPERIMENTAL SECTION

2.1. Samples. Chipped Japanese cedar (CDR) was purchased from a wood-processing company and used as the feedstock for the pyrolysis. The average size and moisture contents of CDR were 10 × 10 × 2 mm and 11.0 wt % wet, respectively. The as-received chips were dried in air at 110 °C for 24 h for removing the moisture prior to the pyrolysis. The elemental composition and ash contents of the dried CDR were as follows: C, 50.9; H, 6.4; N, <0.1; S, <0.01; Cl, <0.01; and ash, 0.47 wt % dry. In the experiments for simulating the HO recycling, HO-loaded CDR, hereafter referred to as HO-CDR, was subjected to the pyrolysis. The method for preparing HO-CDR is described in the following subsections.

2.2. Pyrolysis. Figure 2 shows a schematic diagram of the apparatus that was employed for the pyrolysis experiments. CDR or a HO-CDR was continuously fed into the screw-conveyer pyrolyzer[26] together with atmospheric N_2 (purity > 99.9995 vol %), flowing at a rate of 1.0 L min^{-1} standard temperature and pressure (STP). The feeding rate of CDR was fixed at 4.3 g min^{-1} dry. The feeding rate of HO-CDR was higher than that of CDR (without HO loading) and depended upon its HO loading but fixed at 4.3 g of CDR min^{-1}. The amount of CDR or HO-CDR was 165 g of CDR for every pyrolysis run. The temperature of the pyrolyzer, defined by that inside the hollow shaft of the screw, distributed over a range from 250 °C (at the inlet) to 500 °C (center), along with the axis. From the distance between the inlet and center of the pyrolyzer (150 mm) and the average moving rate of the chips in the axial direction (3.2 mm s^{-1}), the average heating rate of chips was estimated to be 5.3 °C s^{-1}, assuming that the rate of heat transfer from the pyrolyzer wall to pyrolyzing chips was sufficiently high.

The char dropped into the char collector and cooled to ambient temperature. Atmospheric N_2 was continuously supplied to the char collector at a flow rate of 0.5 L min^{-1} STP for avoiding the diffusion of the volatiles into the collector. The vapor of the volatiles was sent to the HO sorber via the L-shaped SUS304 pipe (pipe 1; inner diameter = 40 mm) and the SUS316 pipe (pipe 2; inner diameter =11.7 mm) that were heated at 450 and 300 °C, respectively. The HO sorber consisted of a SUS304-made cylindrical vessel with an inner diameter and depth of 70 and 260 mm, respectively, and it contained a bed of 165 g of dry CDR. This amount was the same as that of the CDR or HO-CDR (on a CDR mass basis) fed to the pyrolyzer. A vertical screw was installed in the sorber and rotated at 8.0 rpm for radial/axial mixing of CDR chips. This mixing was in fact necessary for uniform loading of HO in the sorber. The temperature of the CDR bed was monitored during the pyrolysis

dx.doi.org/10.1021/ef2011673 |*Energy Fuels* 2012, 26, 256–264

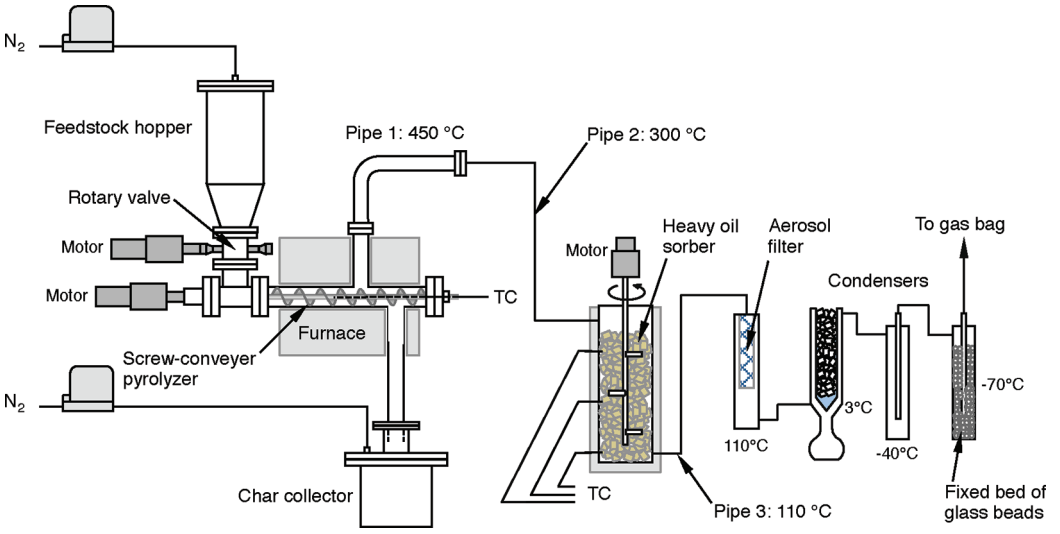

Figure 2. Schematic diagram of the experimental apparatus for pyrolysis. TC = thermocouple.

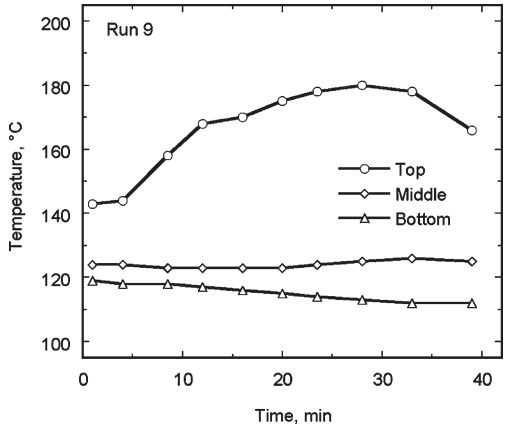

Figure 3. Change in the temperature of the HO sorber with time during a pyrolysis run.

run at its top, middle, and bottom. Typical temperature variations during the pyrolysis are illustrated in Figure 3. The top temperature that was initially 140 °C started to increase when the first volatiles came into the sorber, further increased up to 180 °C, and then decreased because of the termination of CDR or HO-CDR feeding to the pyrolyzer. The middle and bottom temperatures were maintained at 120−130 and 110−120 °C, respectively. The sorber was heated with a mantle heater, so that the bottom temperature was maintained above 110 °C.

The volatiles that had passed through the HO sorber entered a thimble filter made of silica fibers, where aerosol-forming oil was deposited. The temperature of the filter was kept at 110 °C. The stream of volatiles consisting of vaporous LO, steam, and noncondensables was introduced into a train of three condensers cooled at 3, −40, and −70 °C, respectively. The last condenser was packed with glass beads (diameter of 3 mm) for complete condensation and recovery of furan (boiling point of 32 °C) and the other organic products with higher boiling point temperatures. The noncondensable products, i.e., inorganic gases, C_1−C_4 hydrocarbon gases, formaldehyde, and acetaldehyde, were allowed to pass through the condensers and collected in gas-tight bags made of aluminum-coated plastic films. The collected gas was subjected to gas chromatography (GC).

2.3. Definition of HO and LO. HO was defined as a portion of the oil, which was condensed or sorbed in the HO sorber, and its amount

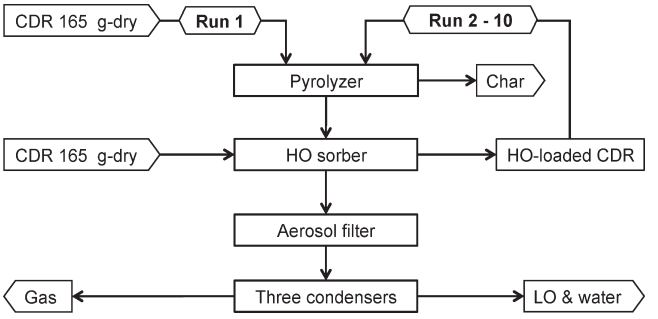

Figure 4. Sequential 10 pyrolysis runs for simulating HO recycling.

was determined by the net increase in the mass of the sorber in the pyrolysis run. The other portions of the oil collected downstream were defined as the constituents of the LO. HO and LO were thus defined experimentally. Some preliminary runs of the pyrolysis of CDR were performed without installing the HO sorber. In other words, the volatiles formed in the pyrolyzer were sent to the aerosol filter via the SUS pipes. The oil condensed in the filer in the form of a black-colored pitch-like half solid accounted for 20.0 wt % dry CDR. On the other hand, when the pyrolysis of CDR was performed with the HO sorber between the pyrolyzer and the filter, the yield of oil condensed in the filter was only 0.5 wt % dry CDR. The oil had an orange color. Such a low yield was due to condensation/sorption of oil by as much as 19.9 wt % dry CDR in the HO sorber. Thus, under the present experimental conditions, the bed of CDR was capable of capturing aerosol-forming oil nearly completely. This was the reason why the HO was experimentally defined, as mentioned above.

2.4. Simulation of HO Recycling. The experimental simulation of the HO recycling consisted of 10 pyrolysis runs in sequence, the diagram of which is shown in Figure 4. In the first run, the dry CDR was pyrolyzed, while HO was condensed/sorbed in the HO sorber. The resulting HO-CDR was used as the feedstock for the second run. The third and later runs were performed in the same manners as the second run. For every pyrolysis run, the yields of char, HO, LO, water, and noncondensable gases were determined. The total recovery of the product, defined by the following equation, was within a range from 98.0 to 101.1%:

$$\text{recovery} = (\text{total mass of char, HO-CDR, HO, LO, water, and noncondensables gas})/(\text{total mass of CDR or HO-CDR fed to the pyrolyzer and that charged in the HO sorber}) \quad (3)$$

dx.doi.org/10.1021/ef2011673 |*Energy Fuels* 2012, 26, 256–264

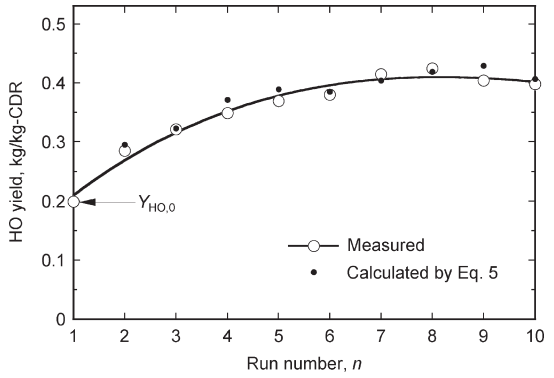

Figure 5. Change in the HO yield with the run number.

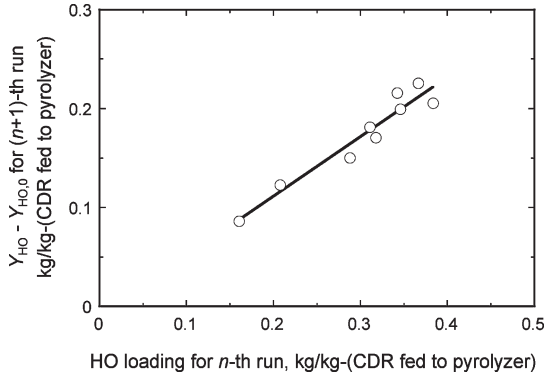

Figure 6. Change in the HO yield with the run number.

The HO loading on the CDR was defined by

$$\text{HO loading} = \frac{\text{mass of HO-CDR}}{\text{mass of dry CDR}} - 1 \quad (4)$$

The HO loading was lower than the HO yield by 0.8−2.0 wt % dry CDR because of condensation of a portion of HO before reaching the bed of CDR. This portion was recovered separately from the HO-loaded CDR and not used for the next run. Water was quantified by Karl Fischer titrimetry. LO was present in both the water and oil phases that were formed in the condensers, and it was then classified into two portions: LO-WP and LO-OP, which contained the water and oil phases, respectively. LO from the condensers was entirely collected and transferred to a separating funnel, and the LO-WP (lower phase) was taken out manually and carefully, so that a drain of LO-OP (upper phase) was avoided. The LO from the 10th run was subjected to thermogravimetric analysis (TGA) and gas chromatography mass spectrometry (GCMS) using a Bruker TG-DTA 2000S and a Shimadzu QP-5000, respectively.

2.5. Analysis of Char. The char sample from the 10th run was subjected to further pyrolysis (i.e., reheating in atmospheric N_2 flow) with a heating rate and peak temperature of 20 °C min^{-1} and 750 °C, respectively. Further oil formation was examined by quantifying aromatic compounds evolved during the heating by a combination of GC and high-performance liquid chromatography (HPLC).[27] It was confirmed that the yields of BTX, phenol, and naphthalene were 0.040, 0.0030, and 0.0033 wt % dry char, respectively. Alkyl phenols, triaromatics, and tetra-aromatics were also quantified, but their total yield was below 10^{-4} wt % dry char. The temperature for the CDR pyrolysis, i.e., 500 °C, was high enough to complete oil evolution from CDR and produce a smokeless char.

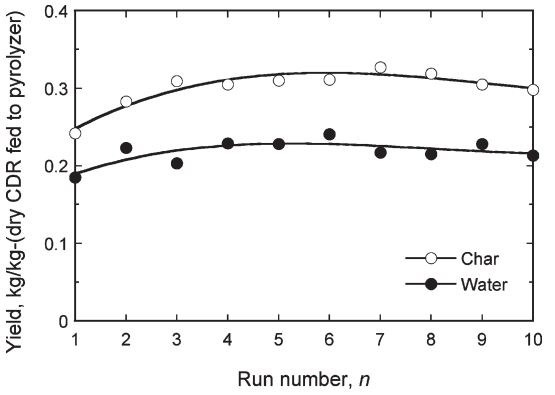

Figure 7. Changes in char and water yields with the run number.

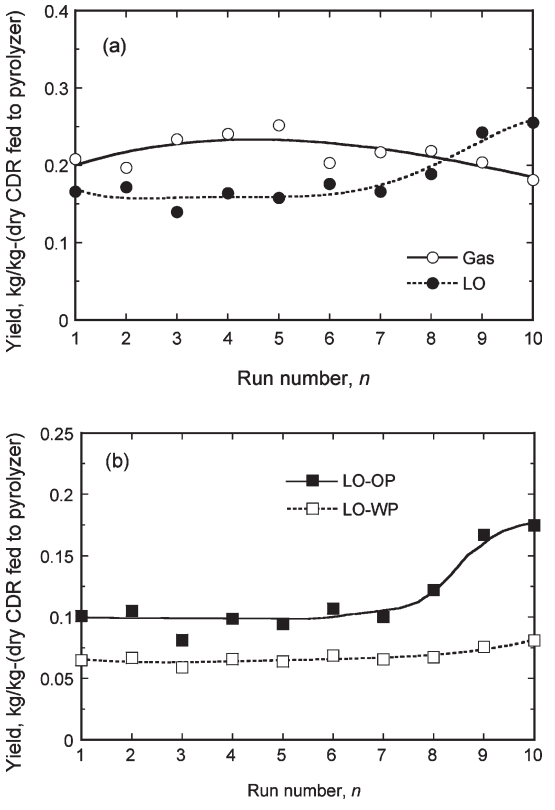

Figure 8. Changes in LO and gas yields with the run number.

3. RESULTS AND DISCUSSION

3.1. Change in the Yield of HO with Progress of Its Recycling. Figure 5 shows the HO yield as a function of the run number from 1 to 10. The HO yield in the first run, which is defined as $Y_{HO,0}$ by eq 1, is 0.199. The yield increases with the run number (n) up to 7 and becomes steady within a range of 0.40−0.42 at n = 7−10. The net conversion of HO retained by the CDR during the pyrolysis, X_{HO}, was estimated from the relationship between the HO loading in nth run and the HO yield in the (n + 1)th run. Figure 6 plots the difference between the HO yield (Y_{HO}) for the (n + 1)th run and $Y_{HO,0}$ against the HO loading for the nth run. The slope of the straight line drawn in this figure has a meaning of average unconverted fraction of the HO that was fed to the pyrolyzer being retained by the CDR, i.e., 1 − X_{HO}.

dx.doi.org/10.1021/ef2011673 |*Energy Fuels* 2012, 26, 256–264

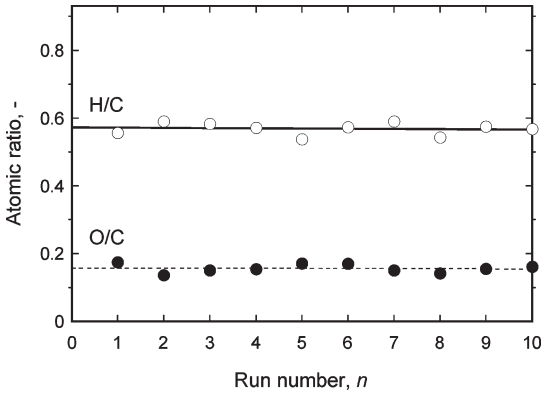

Figure 9. Atomic H/C and O/C ratios of char.

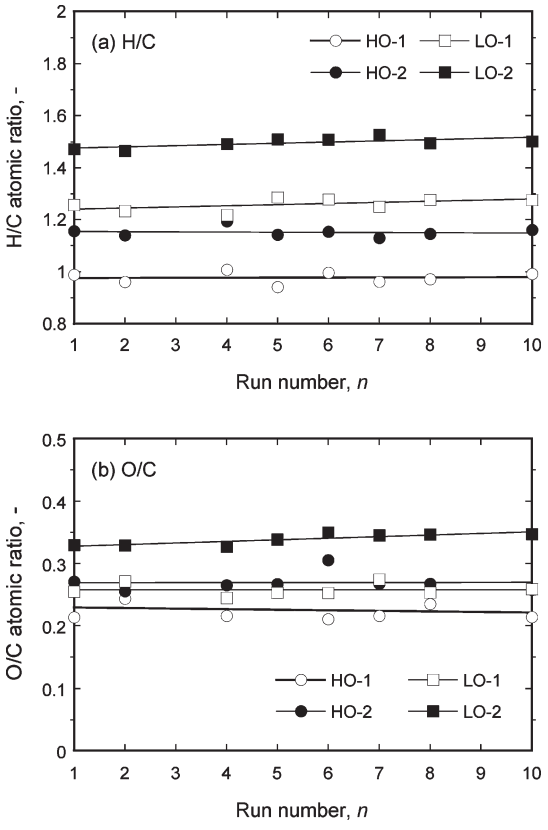

Figure 10. Atomic H/C and O/C ratios of HO and LO. HO-1, HO condensed on the wall of pipe 2; HO-2, HO condensed on the wall of the HO sorber; LO-1, LO deposited in the aerosol filter; and LO-2, LO condensed in the first condenser, forming the oil phase above the water phase.

The average X_{HO} is thus given as 0.40. The dots in Figure 5 indicate the HO yield for the nth run $(n = 2-10)$ that was calculated from the HO loading for the $(n-1)$th run by the following equation assuming that $X_{HO} = 0.4$:

$$Y_{HO} \text{ for the } n\text{th run} = Y_{HO,0} + (1 - X_{HO})\{\text{HO loading for the } (n-1)\text{th run}\} \quad (5)$$

The individual calculated HO yields are in good agreement with the corresponding measured yields. The results shown in

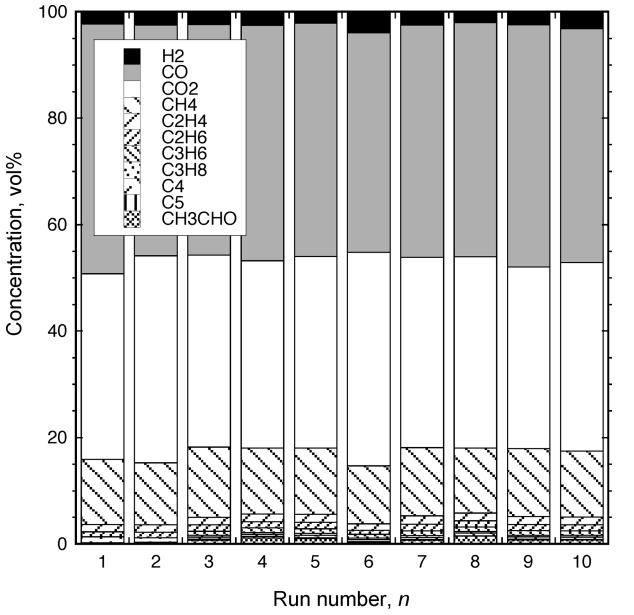

Figure 11. Composition of noncondensable gas.

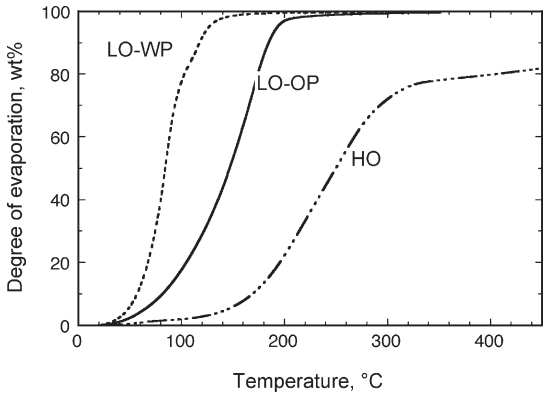

Figure 12. TGA curves for LO-WP (10th run), LO-OP (10th run), and HO. HO was prepared by the pyrolysis of CDR without the HO sorber. The HO was the oil condensed in the aerosol filter with a yield of 20 wt % dry CDR.

Figures 5 and 6 indicate that the HO yield did not continue to increase with the repeated recycling of HO but became steady. Agglomeration of CDR chips hardly occurred even when the HO loading was as high as 0.4 kg/kg of dry CDR. Fractured surfaces of HO-CDR chips were observed, and it was found that HO was not only loaded over the external surfaces but also absorbed into matrices of chips. Although the exact capacity of CDR chips for retaining the HO was unknown, it was safely said that the steady HO loading of around 0.4 kg/kg of CDR was well below the capacity.

3.2. Changes in Yields of LO and Other Products. Yields of the other products changed in manners different from the HO yield. Figures 7 and 8a show the yields of char, water, gas, and LO. The char yield increases from 0.24 to 0.32 kg/kg of dry CDR with the run number up to $n = 6$ or 7 and then decreases slightly to 0.30. Similar trends are seen for the water and gas yields. On the other hand, the LO yield remains steady around 0.16 kg/kg of dry CDR at $n = 1-6$ but increases up to 0.26 at $n = 7-10$.

Table 1. List of Compounds Identified in LO-OP and LO-WP of LO from the 10th Run

number	compound	formula	MW	LO-WP	LO-OP
1	methanol	CH_4O	32.04	×	×
2	acetic acid	$C_2H_4O_2$	60.05	×	×
3	acetone	C_3H_6O	58.08	×	×
4	2-propen-1-ol	C_3H_6O	58.08	×	
5	propanoic acid	$C_3H_6O_2$	58.08	×	
6	2(5*H*)-furanone	$C_4H_4O_2$	84.07	×	×
7	2-butenal	C_4H_6O	70.09	×	×
8	2,3-butanedione	$C_4H_6O_2$	86.09	×	
9	butanoic acid	$C_4H_8O_2$	88.10	×	×
10	butanal	C_4H_8O	72.10	×	
11	propanoic acid, methyl ester	$C_4H_8O_2$	88.10	×	
12	1-hydroxy-2-butanone	$C_4H_8O_2$	88.10	×	
13	1-propanol, 2-methyl-	$C_4H_{10}O$	74.12	×	
14	2-furanmethanol	$C_5H_6O_2$	82.10	×	×
15	3-penten-2-one	C_5H_8O	84.11	×	×
16	2-pentenal, (*E*)-	C_5H_8O	84.11	×	×
17	cyclopentanone	C_5H_8O	84.11	×	×
18	pentanoic acid	$C_5H_{10}O_2$	102.13	×	
19	phenol	C_6H_6O	94.11	×	×
20	furan, 2-acetyl	$C_6H_6O_2$	110.11		×
21	furfural-5-methyl-	$C_6H_6O_2$	110.11		×
22	ethanone, 1-(2-furanyl)-	$C_6H_6O_2$	110.11	×	
23	2-furancarboxaldehyde, 5-methyl-	$C_6H_6O_2$	110.11	×	
24	furan, 2,5-dimethyl	C_6H_8O	96.12	×	×
25	furan, 2,4-dimethyl	C_6H_8O	96.12	×	×
26	2-methyl-2-cyclopentenone	C_6H_8O	96.12		×
27	2-cyclopenten-1-one, 2-methyl-	C_6H_8O	96.12	×	×
28	1,2-cyclopentanedione, 3-methyl-	$C_6H_8O_2$	112.12	×	×
18	cyclohexanone	$C_6H_{10}O$	98.14	×	×
29	3-pentanone, 2-methyl-	$C_6H_{12}O$	100.16	×	×
30	furan, tetrahydro-2,5-dimethoxy-	$C_6H_{12}O_3$	132.15	×	×
31	benzaldehyde	C_7H_6O	106.12		×
32	benzaldehyde, 2-hydroxy-	$C_7H_6O_2$	122.12		×
33	toluene	C_7H_8	92.13		×
34	benzene, methoxy-	C_7H_8O	108.13		×
35	phenol, 2-methyl-	C_7H_8O	108.13	×	×
36	phenol, 3-methyl	C_7H_8O	108.13	×	×
37	phenol, 2-methoxy- (guaiacol)	$C_7H_8O_2$	124.13	×	×
38	2,4-heptadienal, (*E*,*E*)-	$C_7H_{10}O$	110.15		
39	2,3-dimethyl-2-cyclopenten-1-one	$C_7H_{10}O$	110.15		×
40	pentanal, 2,4-dimethyl	$C_7H_{14}O$	114.18	×	×
41	3-hepten-2-ol, (*E*)-	$C_7H_{14}O$	114.18		×
42	cyclohexanone, 3-methyl-	$C_7H_{12}O$	112.17	×	×
43	cyclohexanol, 2-methyl-, *cis*-	$C_7H_{14}O$	114.18		×
44	benzofuran	C_8H_6O	118.13		×
45	styrene	C_8H_8	104.14		×
46	phenol acetate	$C_8H_8O_2$	136.14	×	×
47	2-hydroxy-3-methylbenzaldehyde	$C_8H_8O_2$	136.14		×
48	ethylbenzene	C_8H_{10}	106.16		×
49	*p*-xylene	C_8H_{10}	106.16		×
50	*o*-xylene	C_8H_{10}	106.16		×
51	phenol, 2,6-dimethyl-	$C_8H_{10}O$	122.16		×
52	phenol, 2-ethyl	$C_8H_{10}O$	122.16		×
53	phenol, 2,5-dimethyl-	$C_8H_{10}O$	122.16		×

dx.doi.org/10.1021/ef2011673 |*Energy Fuels* 2012, 26, 256–264

Table 1. Continued

number	compound	formula	MW	LO-WP	LO-OP
54	phenol, 2,3-dimethyl	$C_8H_{10}O$	122.16		×
55	phenol, 4-ethyl	$C_8H_{10}O$	122.16		×
56	phenol, 2-methoxy-4-methyl-	$C_8H_{10}O_2$	138.16		
57	cyclopentene, 1-(1-methylethyl)-	C_8H_{14}	110.19		×
58	hexanal, 2-ethyl	$C_8H_{16}O$	128.21	×	×
59	2-propenal, 3-phenyl- (cinnamylaldehyde)	C_9H_8O	132.15		×
60	benzene, 1-propenyl-	C_9H_{10}	118.17		×
61	ethanone, 1-(3-methoxyphenyl)-	$C_9H_{10}O_2$	150.17		×
62	benzene, 1,2,3-trimethyl-	C_9H_{12}	120.19		×
63	benzene, 1,3,5-trimethyl-	C_9H_{12}	120.19		×
64	2,3-dimethylanisole	$C_9H_{12}O$	136.19		×
65	phenol, 2,4,5-trimethyl-	$C_9H_{12}O$	136.19		×
66	phenol, 2,4,6-trimethyl	$C_9H_{12}O$	136.19		×
67	phenol, 2-ethyl-6-methyl-	$C_9H_{12}O$	136.19		×
68	phenol, 2-propyl-	$C_9H_{12}O$	136.19		×
69	2,3-dimethoxytoluene	$C_9H_{12}O_2$	152.18		×
70	2,6-dimethoxytoluene	$C_9H_{12}O_2$	152.18		×
71	phenol, 4-ethyl-2-methoxy-(*p*-ethylguaiacol)	$C_9H_{12}O_2$	152.18	×	×
72	benzene, (1-methylene-2-propenyl)-	$C_{10}H_{10}$	130.18		×
73	2-propenal, 2-methyl-3-phenyl-	$C_{10}H_{10}O$	146.18		×
74	furan, 2-(2-furanylmethyl)-5-methyl-	$C_{10}H_{10}O_2$	162.18		×
75	benzene, 1-methyl-4-(1-methylethenyl)	$C_{10}H_{12}$	132.20		×
76	benzene, (1-methyl-1-propenyl)-, (*Z*)-	$C_{10}H_{12}$	132.20		×
77	phenol, 2-methyl-6-(2-propenyl)-	$C_{10}H_{12}O$	148.20		×
78	phenol, 2-methoxy-4-(1-propenyl)- (isoeugenol)	$C_{10}H_{12}O_2$	164.19	×	×
79	phenol, 2-methoxy-4-(2-propenyl)- (eugenol)	$C_{10}H_{12}O_2$	164.19		
80	phenol, 2-methoxy-5-[(*E*)-1-propenyl] (*trans-m*-propenyl guaiacol)	$C_{10}H_{12}O_2$	164.19		×
81	phenol, 2,3,4,6-tetramethyl-	$C_{10}H_{14}O$	150.21		×
82	phenol, 2,5-diethyl-	$C_{10}H_{14}O$	150.21		×
83	phenol, 3-methoxy-2,4,5-trimethyl-	$C_{10}H_{14}O_2$	166.21		×
84	phenol, 2-methoxy-4-propyl-(*p*-propylguaiacol)	$C_{10}H_{14}O_2$	166.21		×
85	limonene	$C_{10}H_{16}$	136.23		×
86	naphthalene, 1,5-dimethyl-	$C_{12}H_{12}$	156.22		×
87	naphthalene, 1,2-dihydro-1,1,6-trimethyl-	$C_{13}H_{16}$	172.26		×
88	naphthalene, 1,6-dimethyl-4-(1-methylethyl)-	$C_{15}H_{18}$	198.29		×
89	naphthalene, 1,2,3,4-tetrahydro-1,6-dimethyl-4-(1-methylethyl)-, (1*S-cis*)-	$C_{15}H_{22}$	202.33		×
90	copaene	$C_{15}H_{24}$	204.34		
91	naphthalene, 1,2,4a,5,6,8a-hexahydro-4,7-dimethyl-1-(1-methylethyl)-, (1α,4aα,8aα)-	$C_{15}H_{24}$	204.34		×
92	naphthalene, 1,2,3,5,6,8a-hexahydro-4,7-dimethyl-1-(1-methylethyl)-, (1*S-cis*)-	$C_{15}H_{24}$	204.34		×
93	naphthalene, 1,2,3,5,6,7,8,8a-octahydro-1,8a-dimethyl-7-(1-methylethenyl)-, 1*R*-(1α,7β,8aα)-	$C_{15}H_{24}$	204.34		×
94	1-naphthalenol, 1,2,3,4,4a,7,8,8a-octahydro-1,6-dimethyl-4-(1-methylethyl)-, 1*S*-(1α,4α,4aβ,8aβ)-	$C_{15}H_{26}O$	222.36		×
95	1-naphthalenol, 1,2,3,4,4a,7,8,8a-octahydro-1,6-dimethyl-4-(1-methylethyl)-, 1*R*-(1α,4β,4aβ,8aβ)-	$C_{15}H_{26}O$	222.36		×
96	cedrol	$C_{15}H_{26}O$	222.36		×

The increase in the char yield was primarily attributed to self-charring of the HO retained by the CDR. Pyrolysis of CDR was performed without installing the HO sorber, and the HO was collected with the aerosol filter. It was believed that this HO

dx.doi.org/10.1021/ef2011673 |*Energy Fuels* 2012, 26, 256–264

sample was the best sample representing the HO that was loaded on CDR when the HO sorber was installed. The HO sample was subjected to TGA, and it was found that the HO yielded 20 wt % char during heating to 500 °C. Assuming that the HO and CDR of a HO-CDR underwent pyrolysis independent of the other, the char yield from the HO-CDR was calculated by

$$Y_{\text{char-calcd, HO-CDR}} = Y_{\text{char, CDR}} + 0.2(\text{HO loading to CDR}) \quad (6)$$

In this equation, $Y_{\text{char-calc,HO-CDR}}$ and $Y_{\text{char,CDR}}$ are the char yield calculated by the above equation and the measured char yield from the CDR alone, respectively. Although not shown in detail, it was found for the runs of $n = 2-7$ that $Y_{\text{char-calc,HO-CDR}}$ was approximately equivalent with the measured char yield from the HO-CDR with an average difference of +0.009 kg/kg of dry CDR. This indicated that the increase in the char yield, as seen in Figure 7, was explained mainly by the self-charring. In other words, contribution of the co-pyrolysis of HO and CDR was not so significant as to enhance the char formation greatly. Accordingly, it was believed that the increases in the gas and water yields, as seen in Figures 7 and 8a, were ascribed mainly to the self-pyrolysis of HO. Figure 8a also indicates that the LO yield remains 0.15−0.17 kg/kg of dry CDR at $n = 1-7$ but increases quickly up to 0.26 kg at $n = 8-10$. In the runs of $n = 1-7$, HO retained by CDR was converted to char, water, and gas but little to LO. The sudden and significant increase in the LO yield at $n = 8-10$ was explained by gradual degradation of CDR-retained HO in the runs of $n = 1-7$, which provided an induction period for LO production from HO in the runs of $n = 8-10$. At $n = 8-10$, $Y_{\text{char-calc,HO-CDR}}$ was lower by 0.014−0.015 kg/kg of dry CDR than the measured char yield from HO-CDR. This is an indication of the reduction of the char-forming potential of the CDR-retained HO and consistent with the increase in the LO yield at $n = 8-10$.

Figure 8b shows that the yield of LO-OP increased selectively in the runs of $n = 8-10$. As shown later, LO-OP constituents had a greater average carbon number (number of carbon atoms per molecule) than LO-WP constituents. Thus, the runs of $n = 8-10$ might be in the induction period for producing LO-WP from HO via LO-OP. Compositions and volatility of a set of LO-OP and LO-WP will be shown later.

3.3. Composition of Individual Products. Figure 9 exhibits the H/C and O/C atomic ratios of char and demonstrates that the HO recycling hardly influenced the elemental composition of the char. Similar trends were confirmed for the HO and LO (Figure 10). HO samples were recovered from a SUS pipe between the pyrolyzer and HO sorber (HO-1) and also from the wall of the HO sorber (HO-2, trace amount). LO samples were prepared from its portion condensed in the aerosol filter (LO-1) and another portion condensed in the first condenser, forming an oil phase (LO-2). The H/C and O/C atomic ratios of HO/LO components seemed to be steady over the entire range of the runs of $n = 1-10$, while the ratio of LO-2 slightly increased with the run number. It is noted that the H/C ratios of the four selected oil samples were in the order of LO-2 > LO-1 > HO-2 > HO-1, while the O/C ratios were in the order of LO-2 > LO-1 ≈ HO-2 > HO-1. It thus seemed that an oil component with a lower H/C and O/C ratio was condensed earlier or at a higher temperature. Composition of noncondensable gas was compared among the runs in Figure 11. No significant change in the gas composition occurred along with the run number. The heating values of the gases were in a range from 12.8 to 14.4 MJ/Nm^3 lower heating value (LHV) on a N_2/moisture-free basis.

3.4. Volatility and Composition of LO. According to recent reports on the quick evaluation of bio-oil composition by TGA[28−30] that classifies the bio-oil into components with similar volatilities, the LO-WP and LO-OP from the 10th run were subjected to TGA for examining their volatility. Figure 12 draws TGA curves during heating of the LO-WP and LO-OP at a rate of 5 °C/min under atmospheric flow of N_2 at a rate of 100 mL min^{-1} STP. The content of organic compounds in the LO-WP was 38 wt %. For comparison, a HO sample was subjected to TGA under the same conditions as above. The method for preparing this HO sample was mentioned in a previous section. The LO-WS and LO-OP were evaporated nearly completely until 150 and 250 °C, respectively, while the HO was evaporated more slowly, leaving char with a fraction of about 20 wt %. The volatility of the LO was thus very different from that of the HO in terms of the temperature range and degree of vaporization. In other words, the proposed pyrolysis produced bio-oil (yield from the 10th run; 26 wt % dry CDR) that contained very little amount (<0.2 wt %) of residue after evaporation.

The same LO-WP and LO-OP as above were subjected to GCMS analysis for investigating the molecular compositions qualitatively. The analysis detected and identified 96 organic compounds, most of which were typical compounds and found in recent studies.[28−32] Table 1 lists the identified compounds in the LO-WP and LO-OP. The GCMS identified 39 oxygen-containing compounds in the LO-WP, the carbon numbers of which ranged from 1 (methanol) to 10 (eugenol and isoeugenol). GCMS also detected 87 compounds in the LO-OP, which involved 27 oxygen-containing compounds common with the LO-WP. The carbon number of the major LO-OP constituents distributed from 1 to 12. The LO-OP also contained heavier compounds, such as derivatives of naphthalene and naphthalenol and sesquiterpene, with carbon numbers of 12−15. No compounds with carbon numbers greater than 15 were detected in the LO-OP. In Table 1, more than 10 C_1-C_6 oxygenated compounds are listed as either of LO-WP or LO-OP components. However, this would not necessarily mean those compounds existed in only one of LO-WP and LO-OP. Table 1 lists only compounds that were surely assigned according to mass spectra.

3.5. Consideration of HO Recycling in a General Pyrolyzer. Condensation and sorption of HO onto/into the feedstock biomass can occur in updraft pyrolyzers and gasifiers, in which the volatiles from the pyrolysis are carried by the upward gas and through the top part of the bed consisting of feedstock before exiting. Updraft pyrolyzers are thus candidates of those with HO recycling. However, further studies are needed toward the design of such updraft pyrolyzers, because the HO recycling will require a moving bed that involves a "cool" zone at a temperature of 100−200 °C with a sufficient gas residence time or volume.

4. CONCLUSION

This study proposed the biomass pyrolysis with full recycling of HO for selective production of LO together with char and gas. The concept of this pyrolysis process has been proven by accumulation of the recycled HO no more than 43 wt % of the dry feedstock biomass, chipped cedar, which retained the recycled oil without forming agglomerates. The concept has also been validated by high volatility of the resulting LO as high as 99.8 wt %. The product composition from the last of the 10 sequential pyrolysis runs was as follows: char, 32 wt % of the total

output; noncondensable gas, 19 wt % of the total output; water; 22 wt % of the total output; and bio-oil, 27 wt % of the total output. TGA of the recovered water and oil phases showed nearly complete evaporation of these phases until 150 and 250 °C, respectively. GCMS revealed that the organic compounds contained in the water and oil phases had carbon numbers of 1−10 and 1−15, respectively.

The yield of LO selectively produced by the proposed process is less than 30 wt % of the dry feedstock (excluding water) and lower than the general bio-oil yield (excluding water) from the fast pyrolysis. The proposed process may not necessarily be suitable if the primary purpose of the pyrolysis is to produce bio-oil at a maximized yield. On the other hand, the proposed process is reasonable and effective if the process priority is simultaneous production of bio-oil and char (biochar), in particular, if the bio-oil is applied to processes, such as catalytic steam reforming and upgrading, that are intolerant of coke/carbon formation.

AUTHOR INFORMATION

Corresponding Author

*Telephone: +81-92-583-7796. Fax: +81-92-583-7793. E-mail: junichiro_hayashi@cm.kyushu-u.c.jp.

ACKNOWLEDGMENT

A part of this work was carried out in a Research and Development program that was financially supported by the Ministry of Environment (MOE), Japan. The authors are also grateful to the Funding Program for Next Generation World-Leading Researchers (NEXT Program) established by the Japan Society for the Promotion of Science (JSPS), and Strategic Funds for the Promotion of Science and Technology operated by Japan Science and Technology Agency (JST).

REFERENCES

(1) Scott, D. S.; Piskorz, J.; Radlein, D. *Ind. Eng. Chem. Process Des. Dev.* **1985**, *24*, 581–586.

(2) Radlein, D. The production of chemicals from fast pyrolysis bio-oils. In *Fast Pyrolysis of Biomass: A Handbook*; Bridgwater, A., Czernik, S., Diebold, J., Meier, D., Oasmaa, A., Peacocke, C., Piskorz, J., Radlein, D., Eds.; CPL Press: Newbury, U.K., 1999; pp 164−188.

(3) Oasmaa, A.; Czernik, S. *Energy Fuels* **1999**, *13*, 914–921.

(4) Czernik, S.; Bridgwater, A. V. *Energy Fuels* **2004**, *18*, 590–598.

(5) Mohan, D.; Pittman, C. U., Jr.; Steele, P. H. *Energy Fuels* **2006**, *20*, 848–889.

(6) Huber, G.; Iborra, S.; Corma, A. *Chem. Rev.* **2006**, *106*, 4044–4098.

(7) Meier, D.; Scholtze, B. Fast pyrolysis liquid characteristics. In *Biomass Gasification and Pyrolysis, State of the Art and Future Prospects*; Kaltschmitt, M., Bridgwater, A. V., Eds.; CPL Scientific: Newbury, U.K., 1997; pp 431−441.

(8) Bayerbach, R.; Nguyen, V. D.; Schurr, U.; Meier, D. *J. Anal. Appl. Pyrolysis* **2006**, *77*, 95–101.

(9) Mullen, C. A.; Boateng, A. A.; Hicks, K. B.; Goldberg, N. M.; Moreau, R. A. *Energy Fuels* **2010**, *24*, 699–706.

(10) Peacocke, G. V. C.; Russell, P. A.; Jenkins, J. D.; Bridgwater, A. V. *Biomass Bioenergy* **1994**, *7*, 169–178.

(11) Tzanetakis, T.; Ashgriz, N.; James, D. F.; Thomson, M. J. *Energy Fuels* **2008**, *22*, 2725–2733.

(12) Wang, D.; Czernik, S.; Montané, D.; Mann, M.; Chornet, E. *Ind. Eng. Chem. Res.* **1997**, *36*, 1507–1518.

(13) Wang, D.; Czernik, S.; Chornet, E. *Energy Fuels* **1998**, *12*, 19–24.

(14) Czernik, S.; Evans, R.; French, R. *Catal. Today* **2007**, *129*, 265–268.

(15) Czernik, S.; French, R.; Feik, C.; Chornet, E. *Ind. Eng. Chem. Res.* **2002**, *41*, 4209–4215.

(16) Van Rossum, G.; Kersten, S. R. A.; van Swaaij, W. P. M. *Ind. Eng. Chem. Res.* **2007**, *46*, 3959–3967.

(17) Rioche, C.; Kulkarni, S.; Meunier, F. C.; Breen, J. P.; Burch, R. *Appl. Catal., B* **2005**, *6*, 30–139.

(18) Kechagiopoulos, P. N.; Voutetakis, S. S.; Lemonidou, A. A.; Vasalos, I. A. *Energy Fuels* **2006**, *20*, 2155–2163.

(19) Sharma, R.; Brakhshi, N. *Energy Fuels* **1993**, *7*, 306–314.

(20) Adjaye, J.; Bakhshi, N. *Fuel Process. Technol.* **1995**, *45*, 161–183.

(21) Gayubo, A. G.; Aguayo, A. T.; Atutxa, A.; Aguado, R.; Bilbao, J. *Ind. Eng. Chem. Res.* **2004**, *43*, 2610–2618.

(22) Gayubo, A. G.; Aguayo, A. T.; Atutxa, A.; Aguado, R.; Olazar, M.; Bilbao, J. *Ind. Eng. Chem. Res.* **2004**, *43*, 2619–2626.

(23) Adjaye, J. D.; Katikaneni, S. P. R.; Bakhshi, N. N. *Fuel Process. Technol.* **1996**, *48*, 115–143.

(24) Katikaneni, S. P. R.; Adjaye, J. D.; Bakhshi, N. N. *Energy Fuels* **1995**, *9*, 1065–1078.

(25) Bertero, M.; de la Puente, G.; Sedran, U. *Energy Fuels* **2011**, *25*, 1267–1275.

(26) Hosokai, S.; Norinaga, K.; Kimura, T.; Nakano, M.; Li, C.-Z.; Hayashi, J.-i. *Energy Fuels* **2011**, manuscript submitted.

(27) Matsuhara, T.; Hosokai, S.; Norinaga, K.; Matsuoka, K.; Li, C.-Z.; Hayashi, J.-i. *Energy Fuels* **2010**, *24*, 76–83.

(28) Branca, C.; Blasi, C. D.; Elefante, R. *Energy Fuels* **2006**, *20*, 2253–2261.

(29) Garcia-Perez, M.; Chaala., A.; Pakdel, H.; Kretschmer, D.; Roy, C. *Biomass Bioenergy* **2007**, *31*, 222–242.

(30) Garcia-Perez, M.; Wang, S.; Shen, J.; Rhodes, M.; Lee, W. G.; Li, C.-Z. *Energy Fuels* **2008**, *22*, 2022–2032.

(31) Ingram, L.; Mohan, D.; Bricka, M.; Steele, P.; Strobel, D.; Crocker, D.; Mitchell, D.; Mohammad, J.; Cantrell, K.; Pittman, C. U. *Energy Fuels* **2008**, *22*, 614–625.

(32) Mullen, C. A.; Boateng, A. A. *Energy Fuels* **2008**, *22*, 2104–2109.